University of Thi-Qar Journal of Science (UTJsci)
E-ISSN: 2709-0256, P-ISSN: 1991-8690, Vol. 11, No. 1, Jun. 2024

Optical and Electrical properties of organic Aluminum phthalocyanine based thin films for organic electronics

M. Benhaliliba

Film Device Fabrication–Characterization and Application FDFCA Research Group USTOMB, 31130, Oran, Algeria.
mbenhaliliba@gmail.com
mostefa.benhaliliba@univ–usto.dz

Received: 2024-04-03, Revised: 2024-04-20, Accepted: 2024-04-26, Published: 2024-06-19

***Abstract*—This research emphasizes the optical and electrical properties of organic aluminum phthalocyanine (AlPc) molecule based thin films. The transmittance of such materials presents a narrow peak and valley within a range of 446 nm. Dielectric parameters such as refractive index and extinction coefficient are studied within the UV-Vis-IR range. Optical band gap (Eg) and Urbach energy (Eu) values are determined as 2.6 eV and 33 meV. Based on single oscillator dispersion energy and related parameters such as E_0, E_d, S_0, λ_0, n_0, ε_L, N/m* and ε_∞ .The nonlinear optic (NLO) properties are emphasized and electrical parameters are extracted from current-voltage characteristics of the Au/AlPc/Si/Al heterojunction in dark and room temperature conditions.**

***Keywords*—Al Phthalocyanine, Transmittance Plot, Organic layers, Dispersion, Dielectric constants, NLO, Diode.**

I. Introduction

Organic materials gained a considerable part in electronic devices for solar cells and microelectronics and optoelectronics applications [1]. The Phthalocyanines (Pcs) and metalophthalocyanines (MPcs) can be used in light emitting diodes [2]. Fascinating characteristics of Pcs and MPcs include their strong coloring properties, chemical inertness, thermal and chemical stability, photochemical properties, and semiconductivity and photoconductivity. Consequently, they find several technical uses, including solar cells. Indium phthalocyanine chloride/p-Si solar cell is previously fabricated [3]. The ZnPc-based metal–semiconductor Schottky diode Al/ZnPc/ITO is fabricated by an effusion cell coating unit [4].

Absorption is one of the most important optical properties of the active layer in solar cells. Throughout this research, optical properties of AlPc deposited onto glass substrate are investigated. Transmittance, reflectance and absorbance versus photon wavelength are measured, plotted and parameters like optical bandgap are extracted. Based on Wemple–DiDomenico (WDD) single oscillator model , various dielectric and dispersion parameters are evidenced and related parameters are determined, discussed and compared.

II. Experimental set up

The organic material AlPc thin film is used to fabricate the organic heterojunction diode. The Au/AlPc/p-Si/Al organic heterojunction diode is made-up by thermal evaporation technique using the homemade vacuum NVBJ-300 NANOVAK thermal evaporation system. Firstly, p-type Si substrate with (100) crystal orientation is washed in $5H_2SO_4 + H_2O_2 + H_2O$ solution for 1 min to eliminate organic contamination and then cleaned by H_2O + HCl solution. The substrate is then washed in deionized water and dried by nitrogen (N2). After formation of ohmic contact, 0.02 g of the AlPc powder bought from Sigma-Aldrich are thermally evaporated in vacuum at low pressure. The gold metal is thermally evaporated on AlPc layer as front contact through a shadow mask, having a diameter of 1.5 mm. The evaporation process is carried out in chamber of the NVBJ-300 NANOVAK® vacuum thermal evaporation system. The architecture of molecule showing Al in the center of molecule Pc and the design of our heterojunction diode are depicted in Fig. 1. UV-Vis measurements are carried out using Shimadzu UV-3100 PC. Using Keithely 2400 sourcemeter in dark, the current–voltage (I–V) measurement of Au/AlPc/p-Si/Al heterojunction diode is accomplished from within −3 V, +3 V bias voltage range at room temperature.

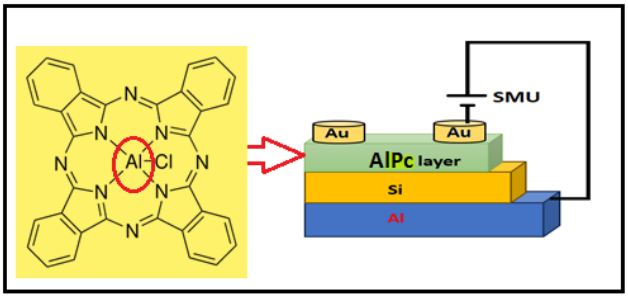

Figure 1: AlPc organic molecule architecture (left) Architecture of Au/AlPc/p-Si/Al diode heterostructure (right).

III. Results and Discussions

https://doi.org/10.32792/utq/utjsci/v11i1.1220

A. *Optical and dispersion properties*

Figure 2 shows the variation of both transmittance T(%) and reflectance R(%) of AlPc organic material based thin film as a function of photon wavelength within the 200-2500 nm range. There is a peak and valley occurrence in the T curve as indicated by rectangle inside a spectral band of 446 nm.

At 315 nm, reflectance of AlPc layer coincides with transmittance at 2.85% as indicated by arrow in inset where the reflectance declines rapidly while transmittance starts to increase from this point inside UV range to attain a peak of 79% at 486 nm then drops till 7% at 790 nm limit of visible band then continues to a highest value of 81 % at 2500 inside IR range. It is observed that change is comprise in a 400-846 nm band. This characteristic might due to optical filter properties as mentioned elsewhere. The reflectance of AlPc thin layer exhibits a decline from UV to VIS and then to IR ranges. It shows a slight peak that looks like a bump as seen in inset of Figure 3. Reflectance R in terms of n and k is expressed as [5-6];

$$R = \frac{(n-1)^2+k^2}{(n+1)^2+k^2} \quad (1)$$

$$k = \frac{\alpha\lambda}{4\pi} \quad (2)$$

Where R (%) is the reflectance, λ is photon wavelength, t is the film thickness and α is the absorption coefficient. The value of t is 673 nm.

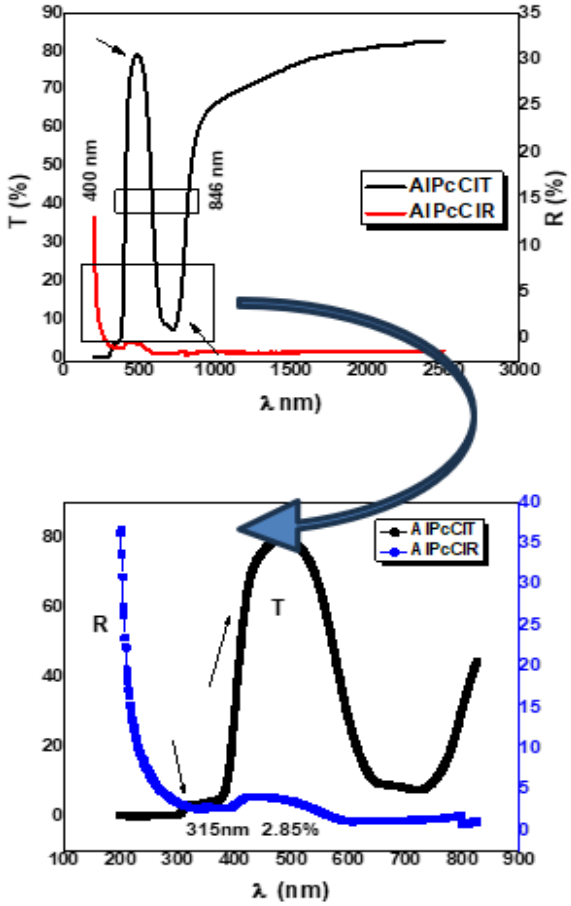

Figure 2: The plot of transmittance and reflectance versus photon wavelength of AlPc layer in double Y axis graph. Arrows spot the peak and valley within the 400-846 visible-near infrared range as indicated by a rectangle.

The extinction coefficient and refractive index as a function of photon wavelength λ, are given by [7];

$$k(\lambda) = \frac{\lambda}{4\pi t}\ln\left[\left[\frac{(1-R(\lambda))^2}{2T(\lambda)}\right] + \sqrt{\left(\left(\frac{(1-R(\lambda))^4}{4(T(\lambda))^2} + (R(\lambda))^2\right)\right.}\right] \quad (3)$$

$$n(\lambda) = \left[\frac{(1+R(\lambda)}{1-R(\lambda)}\right] + \sqrt{\left(\frac{4R(\lambda)}{(1-R(\lambda))^2} - (k(\lambda))^2\right)} \quad (4)$$

$$\alpha(\lambda) = \frac{1}{t}\ln\{\left[\frac{(1-R(\lambda))^2}{2T(\lambda)}\right] + \sqrt{\left(\frac{(1-4R(\lambda))^4}{(4T(\lambda))^2} - (R(\lambda))^2\right)}\} \quad (5)$$

where t is the layer thickness, R and T are reflectance and transmittance. The single-oscillator model of Wimple-DiDomenico (WDD-model) can be used to predict the dispersion parameters of AlPc thin films, such as oscillatory energy, E_o, and dispersive energy, E_d, from the transparent area [8]. In the context of the WDD-model, the refractive index reaction to the photon energy, hυ, can be by eqns. 6-7. In terms of the photon energy E=hν, the energy of the effective dispersion oscillator E_0 and the dispersion energy E_d, the Refractive index of the data is fitted via the expression [8];

$$n^2 - 1 = \frac{E_0 E_d}{E_0^2 - (h\nu)^2} \quad (6)$$

$$n_0^2 = \varepsilon_\infty = \frac{E_0 + E_d}{E_0} \quad (7)$$

where E_0 is oscillator energy, E_d is the dispersion energy, and hν is the photon's energy, h=6.62x10^{-34}J.s is Planck constant [8].

The n^2 in term of λ^2 and N/m* are written as [8-9];

$$n^2 = \varepsilon_L - \frac{e^2}{4\pi^2 c^2 \varepsilon_0}\left(\frac{N}{m^*}\right)\lambda^2 \quad (8)$$

where e is the electron's charge, ε_0 is the vacuum's permittivity, N is the free charge carrier concentration and m* is the charge carrier effective mass.

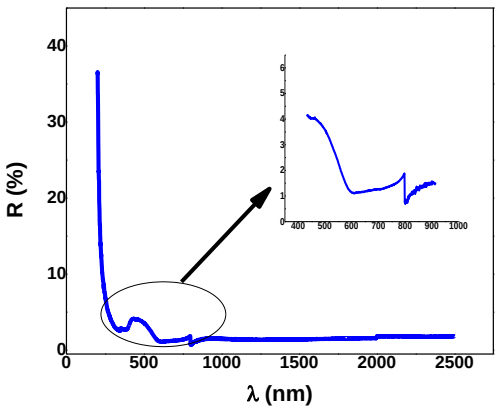

Figure 3: plot of reflectance versus photon wavelength of AlPc layers comparative graph. Inset displays the fluctuation of reflectance within the 400-930 nm visible-near infrared range.

Dielectric constant ε is given by [10];

$$\epsilon = \epsilon_1 - i\epsilon_2 \quad (9)$$

where ε_1 and ε_2 are the real and imaginary parts of complex dielectric constant ε.

$$\epsilon_1 = n^2 - k^2, \quad (10)$$

$$\epsilon_2 = 2nk\,, \quad (11)$$

where n and k are the refractive index and extinction coefficient expressed in eqns. (3-4).
The optical band gap of AlPc thin film is determined by Tauc's law as shown in Figure 4 according to the following equation [6];

$$\boldsymbol{\alpha h\upsilon = A\left(h\upsilon - E_g\right)^n} \quad (12)$$

Where α is absorption coefficient, A is a constant and Eg is the optical band gap, n is a constant exponent which calculates the optical transitions type. For indirect allowed transition, n=2; for indirect forbidden transition, n=3, for direct allowed transition, n= 1/2; for direct forbidden transition, n=3/2. A medium value of bandgap, Eg=2.6 eV, compared to Si (1.12 eV) value and to ZnO (3.5 eV) is obtained. A value greater of Eg, 3 eV, is obtained for N,N′ -Bis(3-methylphenyl)-N,N′ -diphenylbenzidine (TPD) film [11].

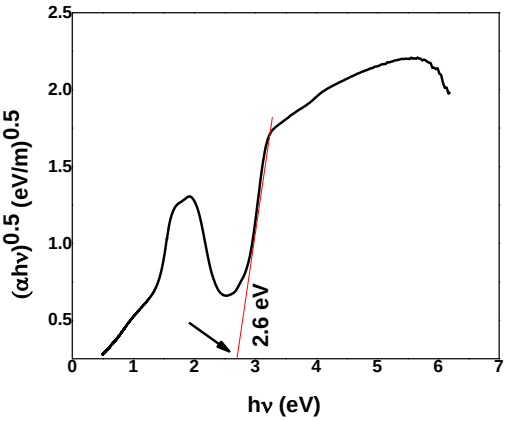

Figure 4: Tauc's plot of AlPc organic layers showing an optical band gap of 2.6 eV as displays by an arrow.

Urbach energy Eu is determined by plotting lnα against energy hν according to the following equation [6];

$$E_u = \frac{dh\upsilon}{dln\alpha} \quad (13)$$

Plotting the linear portion in the ln vs. hν curve (not shown here) yields the Urbach energy Eu (meV). Eu is found by taking the reciprocal of the slope of the linear component of lnα vs. hν within 3.3 eV-4 eV energy range. Eu is much less than Eg, and the ratio of Eu =33 meV to Eg is approximately Eu/Eg ~ 0.012.
To explain the dispersion behavior of AlPc organic molecule based thin layer the mean oscillator power, Thus, using Sellmeier representation of the real dielectric constant in the single oscillator model, the average oscillator strength, So, and the average oscillator wavelength, λo, are computed as follows [9, 11-12];

$$n^2 - 1 = \frac{S_0\lambda_0^2}{1-\left(\frac{\lambda_0}{\lambda}\right)^2} \quad (14)$$

In order to explore the nonlinear optic properties of organic APc molecule containing π-conjugated bonds. The static value of $\chi^{(1)}$ is considered as [9, 11, 13, 14];

$$\chi^{(1)} = \left[\frac{n^2-1}{4\pi}\right] = \frac{E_d E_0}{4\pi\left(E_0^2 - E^2\right)} \quad (15)$$

In transparent area E<<E_0;

$$\chi^{(1)} = \frac{E_d}{4\pi\, E_0} \quad (16)$$

3rd order nonlinear optical susceptibility is expressed as [13];

$$\chi^{(3)} = A\left[\chi^{(1)}\right]^4 = A\left[\frac{n^2-1}{4\pi}\right]^4 \quad (17)$$

where A is a constant around 1.7×10^{-10} esu.
The nonlinear refractive n_2 is determined in terms of $\chi^{(3)}$ as [8, 12];

$$n_2 = \frac{12\pi\chi^{(3)}}{n_0} \quad (18)$$

Figure 5 shows the refractive index variation as a function of photon wavelength of AlPc film. A decay of n is observed from 4 at 200 nm in UV range to 1.24 at 2500 nm in IR band.

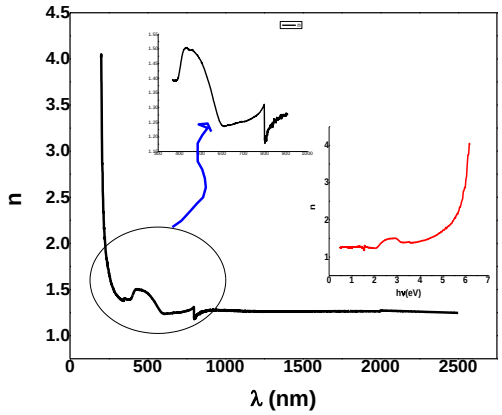

Figure 5: Plot of refractive index of AlPc thin film versus photon wavelength. Inset shows n vs. photon energy and peak occurrence around 500 nm.

A similar decay of n-λ is reported for indigo organic semiconductor film. It is about 1.82 at 900 nm and decreases to 1.68 at 2500 nm [15]. The n-λ curve presents many peaks within 200-500 nm range are revealed by coumarin dye-based metal-free thin films as reported prior [16]. Besides, the optical parameters are recorded as E_0=3.2 eV, E_d= 6.5 eV, ε_L=3.2, ε_∞= 2.99.
Extinction coefficient versus photon wavelength is described in Figure 6. Various peaks are recorded at 224, 483 and 798 nm all inside visible range. Related energies of such are determined (1240/ λ) as 5.53, 2.56 and 1.55 eV as shown in Figure 6. The Figure displays the spectral distribution of refractive index while the inset gives the

photon energy dependence of refractive index. This latter records a growth looks like an exponential progress.

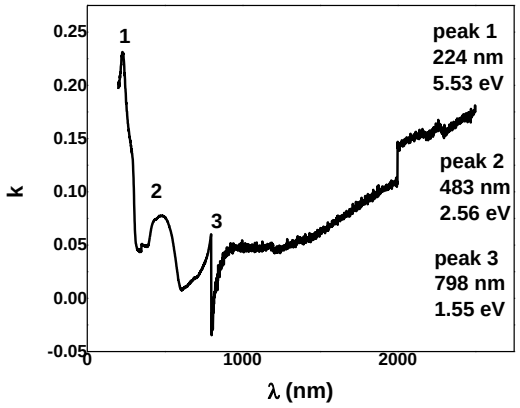

Figure 6: Variation of extinction coefficient of AlPc thin film versus photon wavelength.

Real and imaginary parts of dielectric constant ε_1 and ε_2 of AlPc thin film against photon wavelength are demonstrated in Figures 7-8. It drops from 16.7 to lower values along 500-2500 nm range obeying an exponential decay. A similar decay of ε_2 is followed along 200-2500 nm range from 1.6 to lower values recording weak peaks indicated by arrows as portrayed in Figure 8.

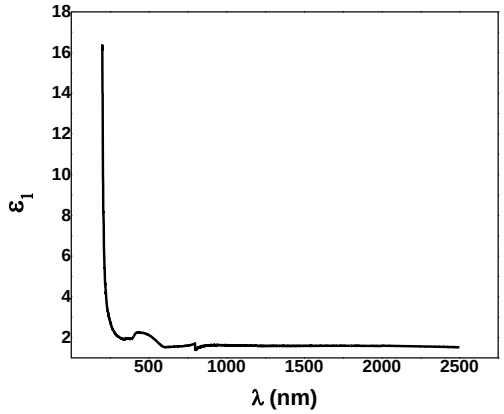

Figure 7: real part of dielectric constant ε1 of AlPc thin film against photon wavelength.

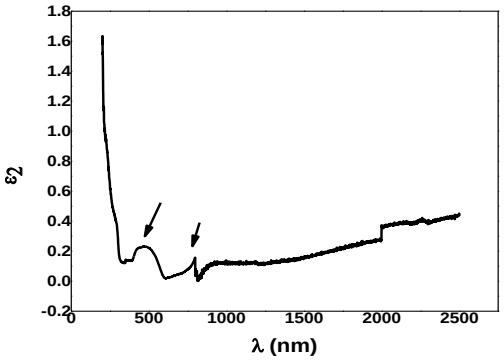

Figure 8: Imaginary part of dielectric constant ε2 of AlPc thin film against photon wavelength

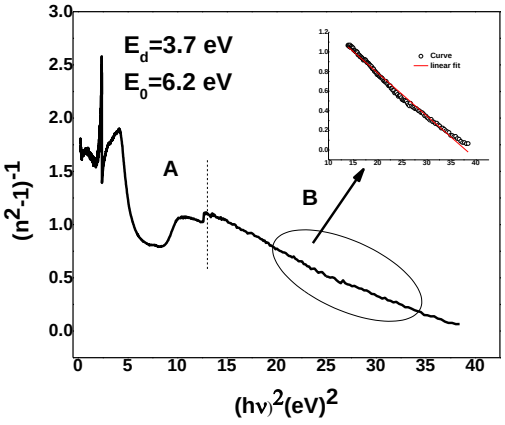

Figure 9: Profile of $(n^2-1)^{-1}$ versus $(h\upsilon)^2$ of AlPc thin film, inset shows the linear portion, Zone B, and linear fit.

The quantity $(n^2-1)^{-1}$ versus $(h\upsilon)^2$ of AlPc thin film is plotted as shown in Figure 9. Two regions are separated fluctuations occurrence in low energy range (A) and a decay looks like a rough straight line (B). By fitting the linear part of $1/(n^2-1)$-1 against $(h\nu)^2$ curve the parameters E_d and E_0 are determined according to eqn. $(n^2-1)^{-1}=E_0/E_d - (h\nu)^2/ E_0E_d$ where the slope is $1/E_0E_d$ and intercept value is E_0/E_d. This latter is 1.66 and $1/E_0E_d$ is 0.043. Consequently, E_0 and E_d are respectively found to be 6.2 eV and 3.7 eV. Where $\varepsilon_\infty=(E_0 + E_d)/E_0$, is found to be 1.59 and n_0 is 1.26. Similar decay of $(n^2-1)^{-1}$ versus $(h\upsilon)^2$ is revealed by Khan for PDS material [8]. PEDOT: PSS exhibits E0 and Ed of 2 and 3.11 eV respectively as Khan et al. reported [8].

2.75 eV and 4.81 eV are the reported values of E_0 and E_d for the Indigo films as mentioned earlier [15].

Lower values, 0.078 and 1.75 are previously cited for MnTPPCl [17] but ZnTPyP exhibits 0.5 eV and 2.84 eV as cited by Shehata et al. [18].

Figure 11 depicts the n^2 versus λ^2 of AlPc organic film plot. An exponential decay is followed by n^2 within $1x10^5$-$4x10^5$ λ^2 range. By fitting the linear part of n^2 vs. λ^2 curve the parameters ε_L and (N/m*) are determined according to $n^2=\varepsilon_L-(e^2N/ 4\pi^2c^2 \varepsilon_0 m^*)\lambda^2$ eqn. where the slope is $e^2N/ 4\pi^2c^2 \varepsilon_0 m^*$and intercept value is ε_L. So, the values of ε_L and N/m* are easily extracted. So, ε_L=1.73, $N/m^*=36x10^{47}$ $kg^{-1}m^{-3}$ are extracted for AlPc organic thin film.

The $1/(n^2-1)$ versus $1/\lambda^2$ of AlPc organic film is drawn as seen in Figure 10. A fluctuation with a decline of $1/(n^2-1)$ is recorded inside region $1/\lambda^2 < 10$ nm^{-2}, beyond this value a linear decay is followed by $1/(n^2-1)$ quantity. By fitting the linear part of $1/(n^2-1)$-1 versus $/\lambda^2$ curve, the parameters S_0 and λ_0 are determined according to eqn. $(n^2-1)^{-1}=1/S_0\lambda_0^2 - (1/S_0)\lambda^{-2}$ where the slope is $1/S_0$ and intercept value is $1/S_0\lambda_0^2$. Intercept is 1.65 and slope is ~66830. Consequently, $S_0=1.5x10^{-5}$ nm^{-2}, λ_0=201.25 nm. Some values of S_0 and λ_0 equal to $1.19x10^{-5}$ nm^{-2} 434 nm are reported previously for Coomassie brilliant blue dye [9].

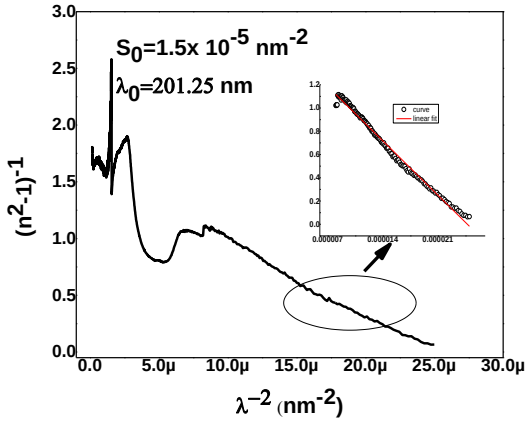

Figure 10: $1/(n^2-1)$ versus $1/\lambda^2$ of AlPc organic film. Inset depicts the linear portion and linear fit as shown by open circle.

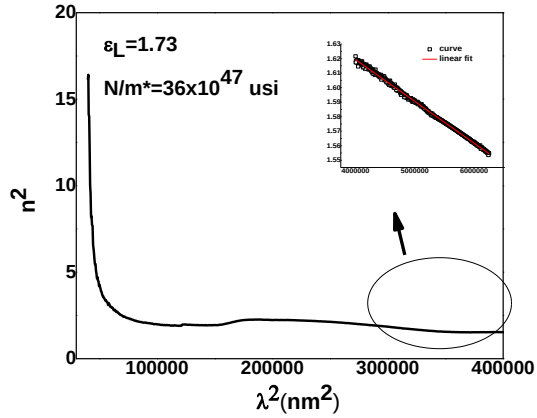

Figure 11: Plotting of n^2 versus λ^2 of AlPc thin film, inset shows the linear portion indicated by open circle and linear fit.

The linear optical susceptibility $\chi^{(1)}$ is resented in Figure 12 for AlPc organic film. Curve is increasing with energy hν till 1.2.

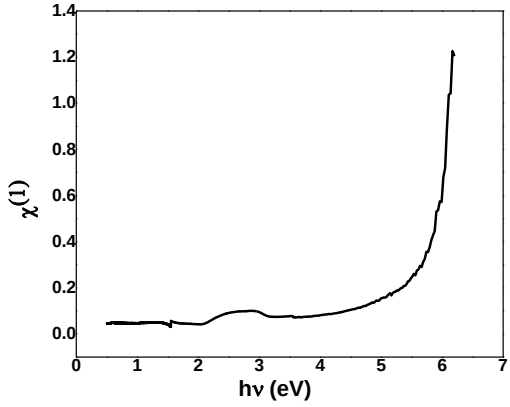

Figure 12: linear optical susceptibility χ(1) of AlPc film versus photon energy.

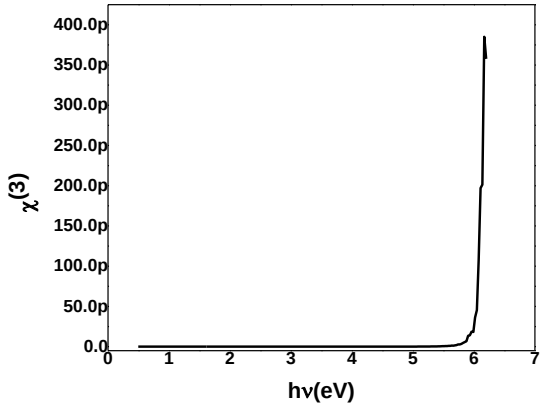

Figure 13: 3rd order nonlinear optical susceptibility χ(3) of AlPc thin layer.

The third order of nonlinear optical susceptibility χ(3) vs. photon energy is displayed in Figure 13. This parameter doesn't change till 6 eV, a rapid growth up to 350p. Similar growth is demonstrated for Indigo film [15].
The values of $\chi^{(1)}$, $\chi^{(3)}$ of organic materials are as follows: 0.14, $0.65x10^{-13}$ esu (Indigo), 2.074 $x10^{-13}$ esu (MnTPPCl), 0.34, 22.6 $x10^{-13}$ esu (ZnTPyP) [15, 17, 18]

B. Electrical measurement

Current-voltage characteristics of our device based AlPc organic thin layer in dark and room temperature conditions are displayed within -3V, +3V bias voltage range as portrayed in Figure 14. Rectifying behavior is important assessed by RR rectifying ratio (RR=I(+3V/-3V)) found to be 80482. Ideality factor is extracted by using of slope in the linear portion expressed as [19];

$$n = \frac{q}{kT}\frac{dV}{d(\ln I)} \qquad (19)$$

where Iand V are the measured current and bias voltage, T is absolute temperature and n is ideality factor which exceeds 1 for non-ideal diode. Electron charge is q and Boltzmann constant is k. Our heterojunction exhibits an ideality factor of 2.35 determined by the slope according to eqn.19 of linear part of I-V curve. This finding reveals that our device is not ideal due to series resistance and interface state. This is shown by curvature of I-V for high voltage as indicated by arrow in Figure 14. Besides, series resistance is around 10 kΩ and barrier height is of 0.74 eV. As reported before, Au/TPD/n-Si/Al heterojunction, TPD is N,N′ -Bis(3-methylphenyl)-N,N′ -diphenylbenzidine, demonstrated lower n~1.4, a barrier height of 0.82 eV and Rs of 20kΩ [11]. Brilliant green dye deposited onto Si heterojunction presents n of 4.3, barrier height of 0.68 in dark [20].

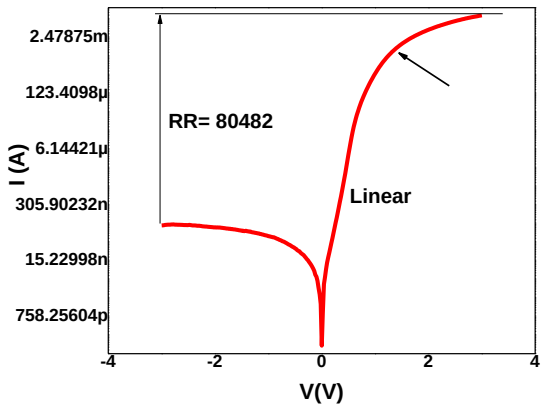

Figure 14: Current-voltage characteistics of Au/AlPc/Si/Al heterostructure in dark and room temperature.

IV. CONCLUSIONS

Throughout this research, a complete study of optical, dielectric, and dispersive properties of AlPc organic material based thin film are investigated. Several optical and dispersion parameters are extracted. Nonlinear properties of AlPc are also studied. As seen from the profile of T/R vs. λ, an exponential decay of R is revealed and both peak and valley within a narrow range are occurred. A medium value of optical bandgap (2.6 eV) and minor Urbach (33 meV) value are easily recorded. A rapid decay of refractive index within UV and approximately a plateau in Vis-IR bands. The sketch of k-λ displays three peaks located at 224, 483 and 798 nm inside UV-Vis ranges.

Using $(n^2\text{-}1)^{-1}$ vs. $(h\upsilon)^2$ plot, 3.7 eV and 6.2 eV are the obtained energies values, oscillator and dispersion energies, of AlPc based thin film. It is concluded a strong decay of both parts of complex dielectric constant ε_1 and ε_2.

Organic material Alpc based thin film exhibits values of S_0 and λ_0 respectively of $1.5x10^{-5}$ nm^{-2} and 201.25 nm using $1/(n^2\text{-}1)$ versus $1/\lambda^2$ curve of AlPc organic film, while the parameters of εL and N/m* are respectively obtained around 1.7 and $36x10^{47}$ usi via the sketch of n^2 vs. λ^2. Nonlinear optic behavior of AlPc organic film is confirmed by the static value of $\chi^{(1)}$ and 3rd order NLO susceptibly $\chi^{(3)}$ values. Both of them exhibit roughly a plateau within 1-6 eV and a rapid growth. Deposited onto Si substrate the heterojunction presents a non-ideal behavior due to resistance and interface occurrence. High rectifying, >80000, of diode based AlPc organic layer is revealed.

Such material can meet several applications in solar cell, OLED, sensors, microelectronic and optoelectronic devices and even organic electronic device applications. Nonlinear properties of AlPc can enlarge its applications.

CONFLICT OF INTEREST

Authors declare that they have no conflict of interest.

REFERENCES

[1] T. Tsuzuki, Y. Shirota, J. Rostaliski, D. Meisner, " The effect of fullerene doping on photoelectric conversion using titanyl phthalocyanine and a perylene pigment", *Sol. Energy Mater. Sol. Cells* 61 pp. 1-8, 2000.

[2] J. Xu, Y. Wang, Q. Chen, Y. Lin, H. Shan, V. A. L. Roy, Z. Xu, "Enhanced lifetime of organic light-emitting diodes using soluble tetraalkyl-substituted copper phthalocyanines as anode buffer layers", *J. Mater. Chem. C* 4, 31, pp.7377–7382, 2016.

[3] H.M. Zeyada, M.M. El-Nahass, E.M. El-Menyawy, A.S. El-Sawah, "Electrical and photovoltaic characteristics of indium phthalocyanine chloride/p-Si solar cell", *Synthetic Metals*, 207, pp.46–53, 2015.

[4] D. Das, M. Das, P. Sahu, P. P.Ray, "Investigation of the metal–semiconductor interface by equivalent circuit model in zinc phthalocyanine (ZnPc) based Schottky diodes and its charge transport properties", *Materials Today: Proceedings*, https://doi.org/10.1016/j.matpr.2023.04.274.

[5] C.E. Benouis, M. Benhaliliba, F. Yakuphanoglu, A. Tiburcio Silver, M.S. Aida, A. Sanchez Juarez, "Physical properties of ultrasonic sprayed nanosized indium doped SnO_2 films", *Synthetic Metals*, 161, pp. 1509– 1516, 2011.

[6] M. Benhaliliba, "ZnO a multifunctional material: Physical properties, spectroscopic ellipsometry and surface examination",*Optik*, 241, p.167197, 2021.

[7] A.M. El-Mahalawy, M.M. Abdou, A.R. Wassel, "Physical and optoelectronic characteristics of novel low-cost synthesized coumarin dye-based metal-free thin films for light sensing applications", *Mater. Sci. Semicond. Process.* 137 p. 106225, 2022.

[8] S. A. Khan, S.Patel , P. Shukla, R.Kumar , R.Dixit, "Synthesis of PEDOT: PSS thin film doped with silver nanoparticles via green approach and study their refractive indices and dispersive parameters using Wemple–DiDomenico (WDD) single oscillator model", *Physica B*, 663, p.414897, 2023.

[9] M. S. Salem, A. R. Wassel, M. Fedawy, A. Shaker, A. H. Al-Bagawia, G. M. Aleid, A. M. El-Mahalawy, "Integration of biocompatible Coomassie Brilliant Blue dye on silicon in organic/Inorganic heterojunction for photodetection applications", *Journal of Physics and Chemistry of Solids* 169, p.110890, 2022.

[10]M. Benhaliliba, T.Asar, I.Missoum, Y.S.Ocak, S.Özçelik, C.E.Benouis, A.Arrar, "Ac Conductivity and Impedance Spectroscopy Study and Dielectric Response of MgPc/GaAs Organic Heterojunction for Solar Energy Application", *Physica B: Condensed MatterPhysica B: Condensed Matter*, 578, 411782, (2020).

[11] A. M. El-Mahalawy, H. Abdel-Khalek , F. M. Amin , M. Abd El Salam, " Dynamics of charge carriers and photoresponse of TPD/n-Si hybrid structure for visible-blind UV self-biased photodetection applications", *Synthetic Metals*, 278, p.116842, 2021.

[12] Ahmed R. Wassel, Eslam R. El-Sawy, Ahmed M. El-Mahalawy, Unveiling of novel synthesized coumarin derivative for efficient self-driven hybrid organic/inorganic photodetector applications, Materials Today Sustainability 26, p.100737, 2024.

[13] A. Stendal, U. Beckars, S. Wilbrand, O. Stenze, C. Von Borczys-kowski, “The linear optical constants of thin phthalocyanine and fullerite films from the near infrared up to the UV spectral regions: estimation of electronic oscillator strength values”, *J. Phys. B Atom. Mol. Opt. Phys.*, 29, pp.2589–2595, 1996.
[14] A.A.M. Farag, A.M. Mansour, A.H. Ammar, M. Abdel Rafea, “Characterization of electrical and optical absorption of organic based methyl orange for photovoltaic application”, *Synth. Met.*, 161, pp.2135–2143, 2011.
[15]S.S. Shenouda, I.S. Yahia, A.M. Shakra, “Linear/nonlinear optical properties and dispersion parameters of nanocrystalline indigo organic semiconductor films”, *Physica B*, 634, p.413787, 2022.
[16] A. M. El-Mahalawy, M. M. Abdou, A. R. Wassel, “Physical and optoelectronic characteristics of novel low-cost synthesized coumarin dye-based metal-free thin films for light sensing applications”, *Materials Science in Semiconductor Processing*, 137, p.106225, 2022.
[17] A.A. Al-Muntaser, M.M. El-Nahass, A.H. Oraby, M.S. Meikhail, “Influence of gamma irradiation on linear and nonlinear optical properties of nanocrystalline manganese (III) chloride tetraphenylporphine thin films”, *Spectrochim. Acta Mol. Biomol. Spectrosc*., 220, p.117112, 2019.
[18] M.M. Shehata, H. Kamal, H.M. Hasheme, M.M. El-Nahass, K. Abdelhady, “Optical spectroscopy characterization of zinc tetra pyridel porphine (ZnTPyP) organic thin films”, *Opt Laser. Technol.*, 106, pp.136–144, 2018.
[19]S.E. Meftah, M. Benhaliliba , M. Kaleli, C.E. Benouis, C.A. Yavru, and A.B. Bayram, “Innovative Organic MEH-PPV Heterojunction Device Made by USP and PVD”, *Journal of Electronic Materials*, 50, No. 4, pp. 2287-2294, 2021
[20] M. Benhaliliba, A. Ben Ahmed, “Innovative Device Based Brilliant Green Dye Material for Optoelectronic and Nonlinear Optic Applications”, *Chemistry Africa*, 7, pp. 1629-1638, 2023.